Since January 2020 Elsevier has created a COVID-19 resource centre with free information in English and Mandarin on the novel coronavirus COVID-19. The COVID-19 resource centre is hosted on Elsevier Connect, the company's public news and information website.

Molecular Immunology 55 (2013) 381–392

Contents lists available at SciVerse ScienceDirect

Molecular Immunology

journal homepage: www.elsevier.com/locate/molimm

Structural basis for the differential classification of HLA-A*6802 and HLA-A*6801 into the A2 and A3 supertypes

Ling Niu[a,b], Hao Cheng[a], Shihong Zhang[a,b], Shuguang Tan[a,b], Yudan Zhang[a,b], Jianxun Qi[a], Jun Liu[a,*], George F. Gao[a,b,c,*]

[a] CAS Key Laboratory of Pathogenic Microbiology and Immunology, Institute of Microbiology, Chinese Academy of Sciences, Beijing, China
[b] University of Chinese Academy of Sciences, Beijing, China
[c] Research Network of Immunity and Health (RNIH), Beijing Institutes of Life Science, Chinese Academy of Sciences, Beijing, China

ARTICLE INFO

Article history:
Received 6 February 2013
Accepted 15 March 2013
Available online 6 April 2013

Keywords:
HLA supertype
HLA-A*6802
HLA-A*6801
HLA-A*0201
T cell

ABSTRACT

High polymorphism is one of the most important features of human leukocyte antigen (HLA) alleles, which were initially classified by serotyping but have recently been re-grouped into supertypes according to their peptide presentation properties. Two relatively prevalent HLA alleles HLA-A*6801 and HLA-A*6802, are classified into the same serotype HLA-A68. However, based on their distinct peptide-binding characteristics, HLA-A*6801 is grouped into A3 supertype, whereas HLA-A*6802 belongs to A2 supertype, similar to HLA-A*0201. Thusfar, the structural basis of the different supertype definitions of these serotyping-identical HLA alleles remains largely unknown. Herein, we determined the structures of HLA-A*6801 and HLA-A*6802 presenting three typical A3 and A2 supertype-restricted peptides, respectively. The binding capabilities of these peptides to HLA-A*6801, HLA-A*6802, and HLA-A*0201 were analyzed. These data indicate that the similar conformations of the residues within the F pocket contribute to close-related peptide binding features of HLA-A*6802 and HLA-A*0201. However, the overall structure and the peptide conformation of HLA-A*6802 are more similar to HLA-A*6801 rather than HLA-A*0201 which illuminates the similar serotype grouping of HLA-A*6802 and HLA-A*6801. Our findings are helpful for understanding the divergent peptide presentation and virus-specific CTL responses impacted by MHC micropolymorphisms and also elucidate the molecular basis of HLA supertype definitions.

1. Introduction

The major histocompatibility complex (MHC) plays a pivotal role in adaptive immune responses by presenting peptides on antigen presenting cell surfaces for subsequent T cell recognition (Goulder and Walker, 2012; Koch et al., 2007; Liu et al., 2011c). For the human MHC, human leukocyte antigen (HLA) alleles possess an extremely high amount of polymorphisms (de Bakker et al., 2006; Marsh et al., 2010). Initially, the HLAs were classified into different serotypes according to their antigenicities (Marsh et al., 2010). Recently, with the identification of numerous peptides that bind to different HLA proteins, the peptide presentation characteristics of HLAs have given rise to a new categorization. HLA molecules with similar peptide binding features are grouped into the same supertypes (Lund et al., 2004; Naugler and Liwski, 2008; Sette et al., 2003; Sidney et al., 1996). Nine major supertypes of HLA class I (HLA I) proteins have been defined based on their shared overlapping peptide-presentation repertoires in the same supertype (Doytchinova et al., 2004a; Reche and Reinherz, 2007; Sette and Sidney, 1998, 1999b; Sidney et al., 2008). Each supertype possesses similar peptide binding motifs.

A2 and A3 are two supertypes with relatively higher frequencies of occurrence (in the range of 39–46% for A2 and 37–53% for A3) among major ethnic groups worldwide compared to other supertypes (del Guercio et al., 1995; Longmate et al., 2001; Zhu et al., 2006). The A2 supertype includes HLA-A*0201 to HLA-A*0207, HLA-A*6802, and HLA-A*6901, etc. These alleles are characterized by a peptide motif of small or aliphatic hydrophobic residues (e.g., Ala, Leu, Ile, Val, Met, Ser, or Thr) at both position 2 and the C-terminal position (Barouch et al., 1995; del Guercio et al., 1995; Doytchinova and Flower, 2002; Fogg et al., 2009; Liu et al., 2010a; Sidney et al., 2001). To date, although most of the defined immunogenic peptide epitopes are with the HLA-A*0201-restriction, dozens of cross-allele-presented peptides have been identified within the A2 supertype (del Guercio et al., 1995; Fogg et al., 2009; Mitchell et al., 2000). The A3 supertype mostly

Abbreviations: HLA I, HLA class I; Pc, C-terminal position of the peptide; P2, position 2 from the N-terminus of the peptide.

* Corresponding authors at: CAS Key Laboratory of Pathogenic Microbiology and Immunology, Institute of Microbiology, Chinese Academy of Sciences, Beijing 100101, China. Tel.: +86 10 64807688; fax: +86 10 64807882.
E-mail addresses: liuj333@gmail.com (J. Liu), gaof@im.ac.cn (G.F. Gao).

0161-5890/$ – see front matter © 2013 Elsevier Ltd. All rights reserved.
http://dx.doi.org/10.1016/j.molimm.2013.03.015

comprises HLA-A*0301, HLA-A*1101, HLA-A*3101, HLA-A*3301, and HLA-A*6801, etc., which present peptides with similar features such as preferences for small or aliphatic residues (e.g., Ala, Leu, Ile, Val, Met, Ser, or Thr) at position 2 and positively charged residues (Arg or Lys) at the C-terminus of the peptides (Doytchinova et al., 2004b; Guan et al., 2003; Hattotuwagama et al., 2007; Sidney et al., 1996).

Interestingly, two relatively common HLA types, HLA-A*6802 and HLA-A*6801, possess only five polymorphic amino acids and belong to the same serotype HLA-A68 (Fernandez-Vina et al., 1992; Marsh et al., 2010). Three of the five polymorphic amino acids locate in the F pocket of the peptide binding groove, while the other two locate in the positions which have no direct effect on peptide binding or T cell recognition (based on the previous TCR-MHC complexes). However, based on their distinct peptide binding properties, HLA-A*6802 and HLA-A*6801 can definitively be grouped into the A2 and A3 supertypes, respectively (Sidney et al., 2008). Elucidation of the molecular basis of the divergent peptide presentation characteristics of HLA-A*6802 and HLA-A*6801, which determine their different HLA supertype classification, requires detailed structural exploration (Gostick et al., 2007). Furthermore, different disease correlation of HLA-A*6802 and HLA-A*6801 was reported (Conway et al., 1997, 1996). It is indicated that HLA-A*6802 allele within the A2 supertype is associated with reduced risk of HIV-1 infection and transmission (MacDonald et al., 2001a, 2000, 2001b; Rowland-Jones et al., 1998). The particularly efficient HIV-specific CTL responses or present epitopes restricted by particular MHC alleles such as HLA-A*6802 may act as one of the restricting elements (Chen et al., 2012; Walker and McMichael, 2011; Wu et al., 2011). However, the association of HLA-A*6801 and HIV infection still remain in debate although it is reported that the HLA-A68 serotype is associated with higher viral load in HIV (Gostick et al., 2007; Ngandu et al., 2009; Tang et al., 2002). Therefore, it is indispensable to characterize the peptide presentation of HLA-A*6802 and perform a comparative analysis with its related allele HLA-A*6801 and HLA-A*0201.

In our previous study, we illuminated the structural basis of cross-allele presentation by HLA-A*0301 and HLA-A*1101 by characterizing their structures complexed to peptide RT313 (Zhang et al., 2011). In this study, we determined the crystal structures of both HLA-A*6802 and HLA-A*6801 complexed with their typically presented peptides, respectively, two of which are HIV-specific antigenic peptides (Env199 and RT313). The structure of HLA-A*6802 complexed with self peptide TRP2-180 derived from a tumor antigen TRP2 was also determined. The binding capabilities of the peptides to HLA-A*6802 and HLA-A*6801, together with HLA-A*0201, were characterized. Our results provide a molecular basis for the supertype differentiation between HLA-A*6801 and HLA-A*6802 and offer a structural reference for understanding HIV-specific T cell immunity among populations with different HLA supertypes (Lichterfeld et al., 2006; Ojesina et al., 2006).

2. Materials and methods

2.1. Peptide synthesis and preparation of the HLA complexes by in vitro refolding

The nonamer peptides Env199 (TLTSCNTSV) derived from human immunodeficiency virus (HIV) Envelope protein (199–207), RT313 (AIFQSSMTK) of HIV reverse transcriptase (313–321), and a human self peptide TRP2-180 (SVYDFFVWL) from Tyrosinase-related protein 2 (180–188) were synthesized (Frahm et al., 2008; Li and Bouvier, 2004; Madden et al., 1993; Parkhurst et al., 1998; Threlkeld et al., 1997; Zhang et al., 2011), and their purity was determined as ~95% by analytical high-performance liquid chromatography (HPLC) and mass spectrometry (Scilight-Peptide, Inc.). The peptides were stored at −80 °C as freeze–dried powders and were dissolved in dimethyl sulfoxide (DMSO) before use. The cDNA of HLA-A*6802 (residues 1–274) was obtained through overlap extension PCR utilizing HLA-A*6801 as a template, which was previously constructed in our laboratory (Gao et al., 2000). The HLA complexes were prepared using in vitro refolding as previously described (Garboczi et al., 1992; Li et al., 2011; Liu et al., 2011b). Briefly, the HLA heavy chain and human β_2m were expressed in inclusion bodies containing in *Escherichia coli* and co-refolded with peptides in a 400 mM L-arginine refolding buffer. Subsequently, the HLA complexes were purified using Superdex® 75 10/300 GL gel filtration chromatography and Resource-Q anion-exchange chromatography (GE Healthcare). Before crystallization, the final buffer was exchanged to 20 mM Tris–HCl (pH 8.0) and 50 mM NaCl.

2.2. Crystallization, data collection, and processing

Crystallization was performed using the hanging drop vapor diffusion technique. Plates were incubated at 291 K and checked for crystal growth one week later. HLA-A*6802/Env199 crystals grown in 0.1 M ammonium acetate, 0.1 M Bis-Tris (pH 6.5), and 17% (w/v) PEG 10,000 at 10 mg/mL. Crystals of HLA-A*6802/TRP2-180 were observed in 100 mM Tris (pH 8.5), and 8% PEG8000 at a protein concentration of 15 mg/mL. Single crystals of HLA-A*6801/RT313 were obtained in a 0.1 M HEPES (pH 7.0) and 30% (v/v) Jeffamine ED-2001 solution with a protein concentration of 10 mg/mL. Diffraction data for HLA-A*6802/Env199 and HLA-A*6802/TRP2-180 were collected at 100 K at the SSRF BEAMLINE BL17U, Shanghai, China at a wavelength of 0.9793 Å. Diffraction data for HLA-A*6801/RT313 were collected using an in-house X-ray source (Rigaku MicroMax007 desktop rotating anode X-ray generator with a Cu target operated at 40 kV and 30 mA) and an *R*-Axis IV++ imaging-plate detector at a wavelength of 1.5418 Å. In each case, the crystal was first soaked in reservoir solution containing 15% glycerol as a cryoprotectant for several seconds and then flash-cooled in a stream of gaseous nitrogen at 100 K. The collected intensities were subsequently processed and scaled using the DENZO program and the HKL2000 software package (HKL Research).

2.3. Structure determination and refinement

The HLA-A*6801/RT313 structure was solved by the molecular replacement method using HLA-A*0301 (Protein Data Bank [PDB] code 3RL1) (Zhang et al., 2011) as the search model in the Crystallography and NMR System (CNS) program (Brunger et al., 1998). The different residues between HLA-A*6801 and the search model HLA-A*0301 were manually rebuilt in the program COOT (Emsley and Cowtan, 2004). Subsequently, restrained refinement was performed using REFMAC5 (Murshudov et al., 1997). Further refinement was performed using the PHENIX software package with isotropic ADP refinement and bulk solvent modeling (Adams et al., 2010). The stereochemical quality of the final model was assessed with PROCHECK (Laskowski et al., 1993). The model of HLA-A*6801/RT313 was subsequently used to determine the structure of HLA-A*6802/Env199 and HLA-A*6802/TRP2-180 by molecular replacement. Crystallographic statistics for the final models of the two complexes are given in Table 1. Figures were generated using PyMOL (http://www.pymol.org/).

2.4. Accession numbers

The accession numbers of HLA-A*6802/Env199, HLA-A*6802/TRP2-180 and HLA-A*6801/RT313 in PDB are 4I48 (http://www.pdb.org/pdb/search/structidSearch.do?structureId=4I48), 4HX1 (http://www.pdb.org/pdb/search/structidSearch.

Table 1
X-ray diffraction data processing and refinement statistics.

	HLA-A*6802/Env199	HLA-A*6802/TRP2-180	HLA-A*6801/RT313
Data processing			
Space group	$P2_1$	C2	$P2_12_12_1$
Cell parameters (Å)			
a (Å)	48.85	129.24	59.63
b (Å)	68.19	37.86	79.04
c (Å)	72.80	108.32	111.15
α (°)	90.00	90.00	90.00
β (°)	100.23	120.04	90.00
γ (°)	90.00	90.00	90.00
Resolution range (Å)	50.00–2.80 (2.90–2.80)[a]	50.00–1.80 (1.86–1.80)	50.00–2.40 (2.49–2.40)
Total reflections	35,687	155,862	146,211
Unique reflections	11,512	41,016	21,190
Completeness (%)	97.7 (99.8)	95.4 (99.9)	99.4 (99.7)
R_{merge} (%)	8.8 (57.8)	5.6 (27.1)	9.5(46.5)
I/σ	12.8 (2.0)	21.7 (4.9)	20.2 (4.1)
Refinement			
R_{work} (%)	21.8	19.0	20.3
R_{free}(%)	28.1	22.6	24.4
r.m.s. deviation			
Bond lengths (Å)	0.003	0.005	0.005
Bond angles (°)	0.756	0.958	0.800
Ramachandran plot quality			
Most favored (%)	88.7	92.3	90.8
Additional allowed (%)	10.7	7.4	8.6
Generously allowed (%)	0.6	0.3	0.6
Disallowed (%)	0	0	0

[a] Values in parentheses are given for the highest resolution shell.

do?structureId=4HX1), and 4HWZ (http://www.pdb.org/pdb/search/structidSearch.do?structureId=4HWZ), respectively.

3. Results

3.1. Overall structures of HLA-A*6802 and HLA-A*6801

The structures of HLA-A*6802 complexed with two peptides Env199 and TRP2-180 were determined to resolutions of 2.8 and 1.8 Å, respectively and the HLA-A*6801/RT313 structure is constructed at a resolution of 2.4 Å (Table 1). As expected, the overall structures of HLA-A*6802 and HLA-A*6801 display the common characteristics of other structurally determined HLA I proteins including the previously determined HLA-A*6801 and HLA-A*0201 structures (Fig. 1A–C) (Bjorkman et al., 1987; Guo et al., 1992, 1993). The extracellular region of HLA-A*6802 heavy chain folds into three different domains: a typical MHC molecule superfamily domain formed by the α1 and α2 domains, and an immunoglobulin like α3 domain which underpins the α1 and α2 domains together with β-microglobulin. The peptides lie along the peptide binding groove formed by two α-helices and eight β-sheets within the α1 and α2 domains.

The overall structure of HLA-A*6802 is extremely similar to that of HLA-A*6801, with a root mean square deviation (RMSD) of 0.784 Å when the whole molecule of HLA-A*6801/RT313 was superimposed with HLA-A*6802/Env199 (Fig. 1D up left and down left). However, the superposition of the structure of HLA-A*6802/Env199 with the previously determined HLA-A*6802/Env199 structure generated an RMSD of 1.536 Å (Fig. 1D up right and up down) (Madden et al., 1993). This is concordant with the higher identity of the amino acid sequences of HLA-A*6802 aligned to HLA-A*6801 (98.2%) than the identity between HLA-A*6802 and HLA-A*0201 (95.6%) (Fig. 2A). Crystal packing of the molecules within these structures has not direct interactions through the HLA helices and thus does not affect the overall structures. The structural alignments of the HLA-A*6801 and HLA-A*6802 with the previously determined HLA-A*6801 and HLA-A*0201 structures also illuminate the similar overall structures of HLA-A*6802 and HLA-A*6801 but not HLA-A*0201. This may indicate a comparable antigenicity between HLA-A*6802 and HLA-A*6801, which gives rise to the similar serotype classification of these two alleles. Furthermore, there are six polymorphic residues between HLA-A*0201 and HLA-A*6801, and HLA-A*6802 that are exposed to the solvent (Supplemental Fig. 1). The solvent-exposed amino acid may locate in the serological recognition of the HLA molecules. Four out of the six polymorphic residues are conserved between HLA-A*6801 and HLA-A*6802, but different from HLA-A*0201, which may contribute to the different serological typing of HLA-A*6801/6802 and HLA-A*0201. HLA-A*6801 has been indicated to be a weak binder for CD8αα due to a polymorphic residue V245, which has previously been observed to change the conformation of the 223–229 loop region in α3 domain. This conformation shift of the 223–229 loop is also observed in HLA-A*6802 structure compared to HLA-A*0201 which may indicate a weak CD8αα binding for HLA-A*6802.

The electron densities for the three bound peptides are well-defined inside the peptide binding grooves of HLA-A*6802 and HLA-A*6801, respectively (Fig. 1A–C). All the peptides utilize residues in position 2 (P2) from the N-terminus and residues at their C-terminus (Pc) as the primary anchors with similar conformations (Leu for Env199, Val for TRP2-180 and Ile for RT313 at P2; Val for Env199, Leu for TRP2-180 and Lys for RT313 at Pc). The crystal packing of the molecules from different asymmetric units of the HLA-A*6802 and HLA-A*6801 structures showed that the adjacent packed molecules have no contact with the peptides, which may indicate the structures determined herein display a natural peptide presentation.

3.2. The peptide presentation of HLA-A*6802 is similar to HLA-A*6801 but not HLA-A*0201

The structure of peptide Env199 complexed with HLA-A*0201 has been determined previously (Madden et al., 1993), which make it possible to compare the peptide presentation of HLA-A*6802

Table 2
Hydrogen bonds and Van der Waals interactions between peptides and HLA residues.

Complex	Peptide		HLA-A*6802		HLA-A*0201	
	Residue	Atom	Hydrogen bond residue (atom)	Van der Waals contact residues	Hydrogen bond residue (atom)	Van der Waals contact residues
Env199	Thr1	N	Tyr171(OH)	Tyr7,Tyr59,Arg62,Asn63,Tyr159,Trp167,Tyr171	Tyr171(OH)	Met5,Tyr7,Tyr59,Glu63,Lys66,Tyr159,Thr163,Trp167,Tyr171
		N			Tyr7(OH)	
		O	Tyr7(OH)		Tyr7(OH)	
		O			Tyr159(OH)	
		OG1			Glu63(OE2)	
	Leu2	N	Asn63(OD1)	Tyr7,Tyr9,Met45,Asn63,Asn66,Val67,Tyr99,Tyr159	Glu63(OE1)	Tyr7,Phe9,Met45,Glu63,Lys66,His70,Tyr99,Tyr159
		N			Glu63(OE2)	
		O			Lys66(NZ)	
	Thr3	N	Tyr99(OH)	Asn66,Tyr99,Trp156,Tyr159	Try99(OH)	Lys66,His70,Tyr99,Tyr159
		O	Asn66(OH)		His70(NE2)	
	Ser4			Asn66		Arg65,Lys66,Gln155
	Cys5			Gln70,Gln155,Trp156		His70,Thr73,Gln155
	Asn6	OD1	Ala69(O)	Ala69,Gln70,Thr73		Thr73
		OD1	Gln70(N)			
		ND2	Thr73(OG1)			
		ND2	Gln70(OE1)			
	Thr7			Asp77,Trp147,Val152		Thr73,Arg97,Trp147,Val152
	Ser8	O	Trp147(OE1)	Val76,Asp77,Lys146,Trp147	Trp147(NE1)	Thr73,Val76,Asp77,Thr80,Lys146,Trp147
		OG	Asp77(OD1)		Asp77(OD1)	
	Val9	N	Asp77(OD1)	Asp77,Thr80,Leu81,Tyr84,Tyr116,Thr143,Lys146,Trp147	Asp77(OD1)	Asp77,Thr80,Leu81,Tyr84,Tyr116,Tyr123,Thr143,Lys146,Trp147
		O	Tyr84(OH)		Lys146(NZ)	
		O	Thr143(OG1)			
		OXT			Tyr84(OH)	
		OXT			Thr146(NZ)	
		OXT			Thr143(OG1)	
	Peptide		HLA-A*6801			
RT313	Ala1	N	Tyr171(OH)	Met5,Tyr7,Tyr59,Asn63,Tyr159,Trp167,Tyr171		
		N	Tyr7(OH)			
		O	Tyr159(OH)			
	Ile2	N	Asn63(OH)	Tyr7,Tyr9,Met45,Asn63,Asn66,Val67,Tyr99,Tyr159		
	Phe3	N	Tyr99(OH)	Asn66,Tyr99,Gln155,Trp156,Tyr159		
	Gln4	OE1	Arg62(NH1)	Arg62,Asn66		
		OE1	Asn66(ND2)			
		NE2	Arg62(NE)			
		NE2	Arg62(NH1)			
		NE2	Arg62(NH2)			
	Ser5	OG	Gln155(OE1)	Gln70,Gln155		
	Ser6	O	Thr73(OG1)	Ala69,Gln70,Thr73		
		OG	Thr73(OG1)			
	Met7			Thr73,Lys146,Trp147,Ala150,Val152		
	Thr8	O	Trp147(OE1)	Thr73,Val76,Aap77,Lys146,Trp147		
	Lys9	O	Tyr84(OH)	Asp77,Thr80,Leu81,Tyr84,Ile95,Arg114,Asp116,Tyr123,Thr143,Lys146,Trp147		
		O	Thr143(OG10			
		N	Asp77(OD1)			
		NZ	Asp116(OD2)			

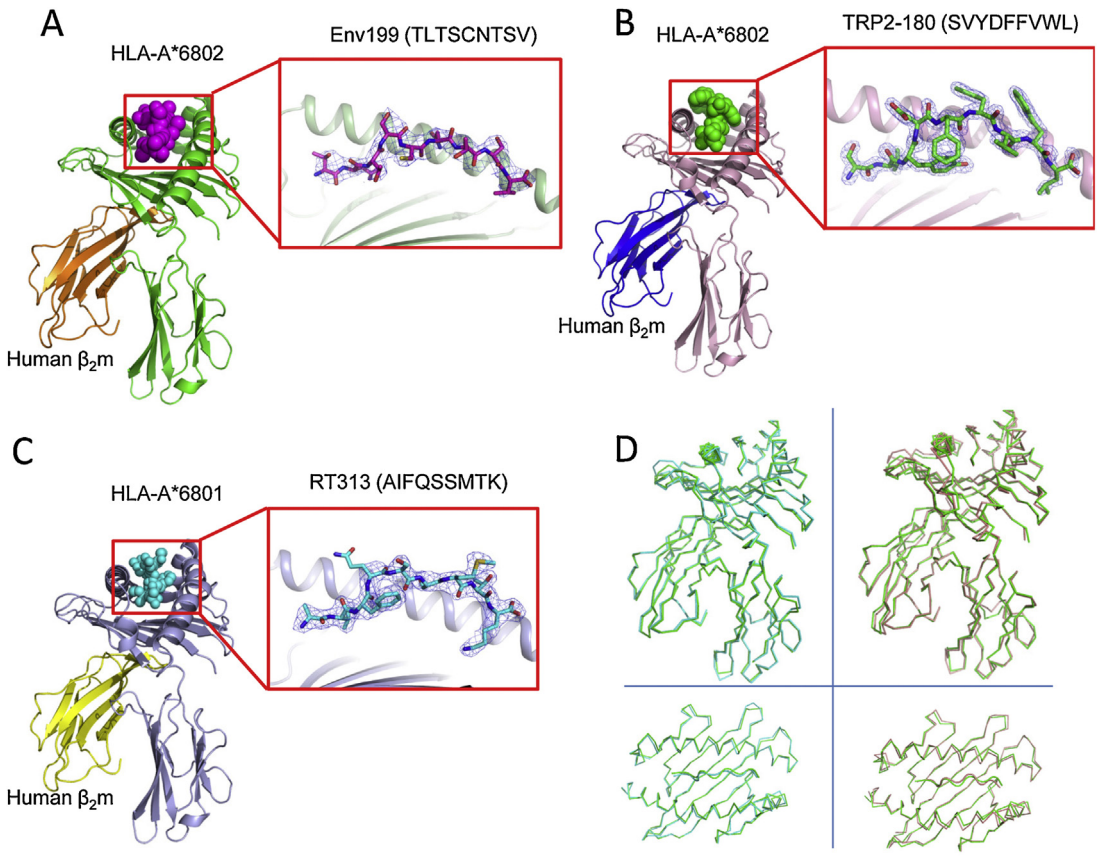

Fig. 1. Overall structures of the HLA-A*6802 and HLA-A*6801 complexes. (A–C) Overview of the structures of HLA-A*6802/Env199 (A), HLA-A*6802/TRP2-180 (B), and HLA-A*6801/RT313 (C) displaying the typical structural conformations of the MHC I molecule. The electron densities of peptides Env199, TRP2-180, and RT313 show their authentic conformations in the HLA grooves. Displayed here are final 2Fo-Fc-stimulated annealing omit maps contoured at 1.0σ. (D) The superpositions of the structures of HLA-A*6802/Env199 (green) with HLA-A*6801/RT313 (cyan, right) and HLA-A*0201/Env199 (pink, right, PDB code 1HHG) show the similar overall structures of HLA-A*6802, HLA-A*6801, and HLA-A*0201.

and HLA-A*0201 using the similar peptide (Table 2). The main chain conformation of the peptides presented by HLA-A*6802 and HLA-A*0201, together with HLA-A*6801 are similar. However, the residues in the middle portion of the peptide Env199 presented by HLA-A*6802, is different from the Env199 presented by HLA-A*0201 (Fig. 3A). The HLA-A*0201-presented peptide Env199 adopts a bulged conformation, with the P6 residue Asn pointing out of the groove. In contrast, the peptide Env199 in the HLA-A*6802 groove presents a flat conformation, with the P6 residue Asn protruding toward the α1-helix.

Due to the different peptide motif preference, we failed in the refolding the HLA-A*6802 and HLA-A*6801 with the same peptides. We determined the structures of HLA-A*6802 and HLA-A*6801 with different peptides: Env199 and RT313, respectively. We found that the main chain conformation and the orientations of residue side chains are extremely similar between the two peptide presented by HLA-A*6802 and HLA-A*6801 (Fig. 3B and C). Both the P6 residues of the two peptides (Asn for Env199, Ser for RT313) point their side chains to the α1-helix (Fig. 3C). The P6-Asn of Env199 and P6-Ser of RT313 form hydrogen bonds with the residues on the α1-helix, e.g. Gln70 and Thr73 which are conserved between HLA-A*6802 and HLA-A*6801 (Figs. 2A and 3D). This indicates a secondary anchor role for hydrophilic residues at the P6 position of the peptides presented by HLA-A*6802 and HLA-A*6801. However, for HLA-A*0201, the hydrophilic residue P6-Asn of Env199 does not form any contact polymorphic residue His70 (Fig. 2A), but protrude upward (Fig. 3C and D), which is concordance with the previous conclusion that the HLA-A*0201 usually has a hydrophobic secondary anchor at P6 position to poke into the groove. The hydrophilic residue such as Asn will be repelled out of the hydrophobic C pocket of HLA-A*0201.

3.3. F pockets with distinct static electrical statuses govern the divergent peptide binding motifs of HLA-A*6802 and HLA-A*6801

Previous studies have elucidated that HLA-A*6802 prefers peptides with the typical HLA-A*0201-restricted peptide motif that is different from the one of HLA-A*6801 (Barouch et al., 1995; del Guercio et al., 1995). Herein, we utilized an in vitro refolding assay to analyze the binding capabilities of HIV peptides Env199 and RT313 to HLA-A*6802, HLA-A*6801, and HLA-A*0201. The typical A2 supertype peptide Env199 facilitated the renaturation of both HLA-A*6802 and HLA-A*0201 but not HLA-A*6801 into soluble complexes reflected by the lack of refolded protein. In contrast, RT313 with its classical A3 supertype peptide motif assisted the refolding of HLA-A*6801 but displayed no binding to either HLA-A*6802 or HLA-A*0201 (Fig. 4A and B).

Peptides Env199 and RT313 have similar aliphatic P2 anchors (Leu in Env199 and Ile in RT313) but differently-charged Pc anchors (Val in Env199 and Lys in RT313). This implies that the F pockets of the three HLA alleles HLA-A*6802, HLA-A*6801, and HLA-A*0201, which accommodate the Pc anchor residues, may contribute to their different binding affinities for the TRP2-180 and RT313 peptides. Structural analysis indicated that the static electrical statuses of the HLA-A*6802 and HLA-A*0201 F pockets are quite different from HLA-A*6801 (Fig. 4C–E). HLA-A*6802 and HLA-A*0201 bear highly hydrophobic F pockets, while HLA-A*6801 possesses a negatively charged F pocket. The F pockets

A

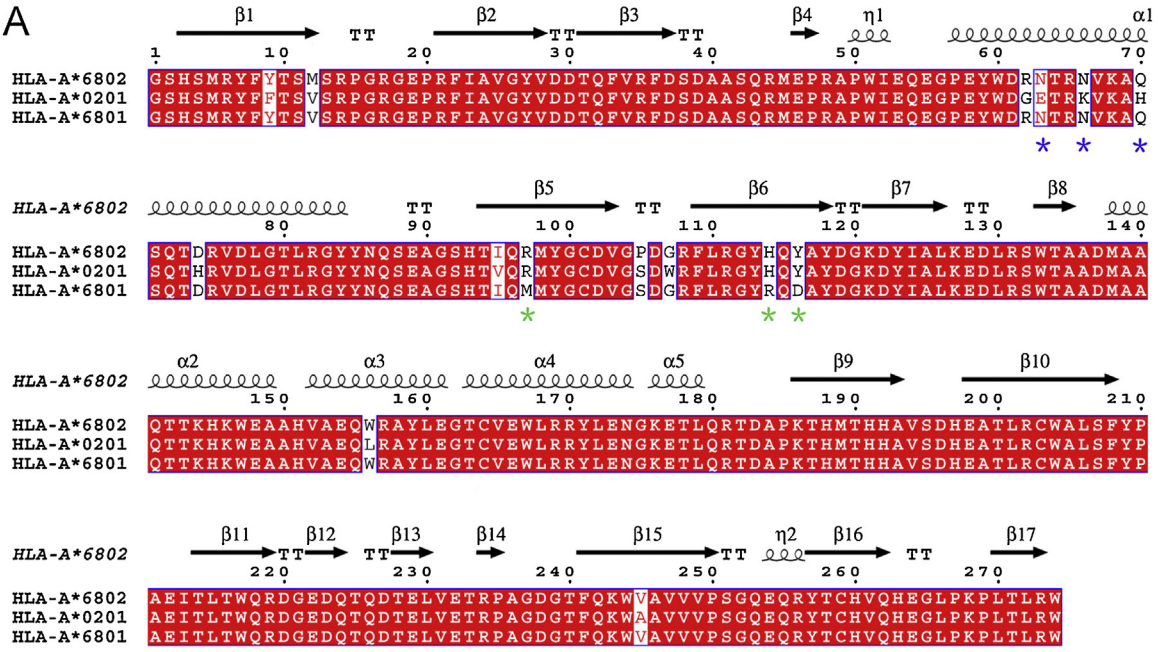

B

		B/C pocket			F pocket		
		63	66	70	97	114	116
Group 1	HLA-A*0201	E	K	H	R	H	Y
	HLA-A*0202	E	K	H	R	H	Y
	HLA-A*0203	E	K	H	R	H	Y
	HLA-A*0204	E	K	H	R	H	Y
	HLA-A*0205	E	K	H	R	H	Y
	HLA-A*0206	E	K	H	R	H	Y
	HLA-A*0207	E	K	H	R	H	Y
	HLA-A*0209	E	K	H	R	H	Y
	HLA-A*0285	E	K	H	R	H	Y
	HLA-A*0286	E	K	H	R	H	Y
Group 2	HLA-A*6802#	N	N	Q	R	H	Y
	HLA-A*6815#	N	N	H	R	H	Y
	HLA-A*6827#	N	N	Q	R	H	Y
	HLA-A*6828#	N	N	Q	R	H	Y
	HLA-A*6831	N	N	H	R	H	Y
	HLA-A*6834	N	N	Q	R	H	Y
	HLA-A*6840	N	N	Q	R	H	Y
	HLA-A*6844	N	N	Q	R	H	Y
	HLA-A*6848	N	N	Q	R	H	Y
	HLA-A*6849	N	N	Q	R	H	Y
	HLA-A*6901#	N	N	Q	R	H	Y

Fig. 2. Polymorphism analysis of HLA-A*6802, HLA-A*6801 and HLA-A*0201. (A) Structure-based sequence alignment of HLA-A*6802, HLA-A*6801 and HLA-A*0201. Cylinders indicate α-helices, and black arrows indicate β-strands. Residues highlighted in red are completely conserved. The key polymorphic residues within the F pockets of HLA-A*6802 and HLA-A*6801 are marked with green asterisks. The key polymorphic residues within the B/C pockets of HLA-A*6802 and HLA-A*0201 are marked with blue asterisk. The sequence alignment was generated with Clustal X and ESPript. (B) Two groups of A2 supertype alleles based on the match of structurally-determined key residues conferring HLA-A*0201-like and HLA-A*6802-like polymorphisms. The representative F pocket residues (green) Arg97, His114, and Tyr116 as in (A) retain the same in all the A2 supertype alleles. In contract, in the B/C pockets, the A2 supertype alleles from "Group 1" have residues Glu63, Lys66, and His70, while the "Group 2" alleles possess Gln63, Gln66 and Asn70, with only His70 of HLA-A*6815 and HLA-A*6831 as exception. #: HLA-A*6815, HLA-A*6827, HLA-A*6828, and HLA-A*6901 are defined into the A2 supertype previously based on the previous experimental or bioinformatic studies. Other alleles are listed in A2 supertype herein according to the prediction based on the key residues in F pocket determined in our structures.

of HLA-A*6802 and HLA-A*0201 are formed by nearly identical residues, which include the similar hydrophobic residue Tyr116 located exactly at the bottom of the F pocket (Fig. 4F). However, the residues composing the F pocket of HLA-A*6801 are quite different, characterized by a negatively charged Asp116 forming a tight salt bridge with the Pc anchor Lys of RT313 (Fig. 4G). Although there are only five polymorphic residues between HLA-A*6802 and HLA-A*6801 (Arnett and Parham, 1995), three of them are located in the F pocket, which leads to a divergent peptide selection of these two closely related HLA alleles within the same serotype.

3.4. B pockets of HLA-A*6802 and HLA-A*6801 subtly differed to HLA-A*0201

Previous studies indicated that the peptides presented by A2 and A3 HLA alleles have the small and aliphatic residues (Ala, Ser, Thr, Val, Leu, Ile, Met) for the P2 primary anchor in the B pocket of the peptide binding groove (Sette and Sidney, 1999a; Sidney et al., 2008). The three peptides we studied here possess the typical residues (Val, Leu, and Ile) for the P2 anchor. This identical P2 anchor preference of HLA-A*6802, HLA-A*6801, and HLA-A*0201 imply a largely similar B pocket formation of the three alleles. Based

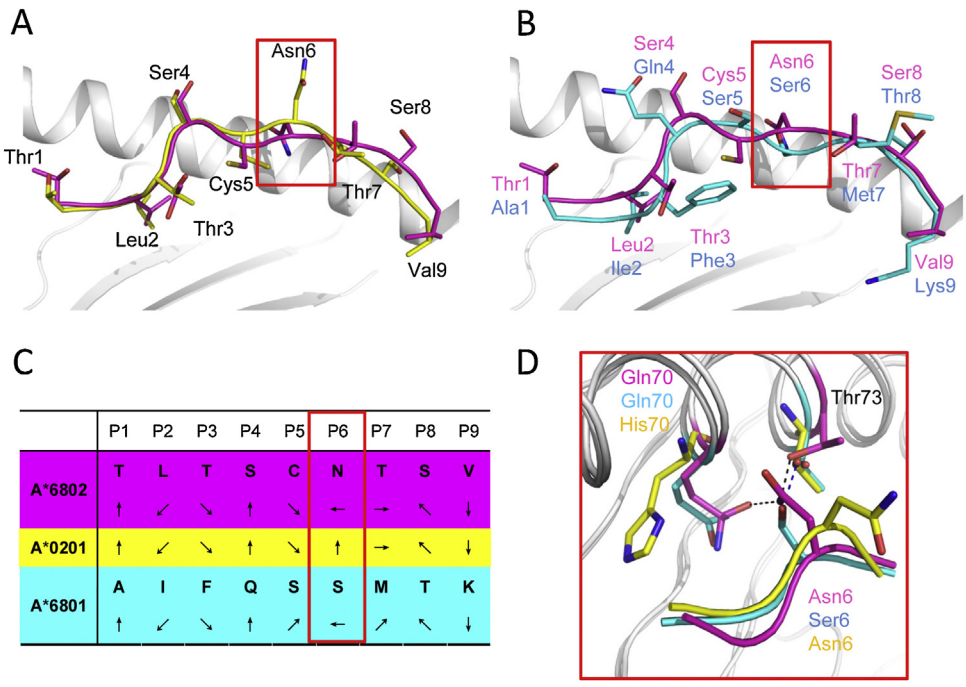

Fig. 3. Comparative alignment of peptides presented by HLA-A*6802, HLA-A*6801 and HLA-A*0201. (A) Superimposition of peptide Env199 (purple) presented by HLA-A*6802 and HLA-A*0201 (PDB code 1HHG), respectively. The different conformations of the main chains occur in the middle portion of the two peptides (P6 positions). (B) Superimposition of HLA-A*6802-presented peptide Env199 (purple) with RT313 (cyan) from the HLA-A*6801 structure. Similar main chain conformation and the side chain orientation of the residues within these two peptides are observed. (C) Side chain orientation for the the peptides presented by HLA-A*6802, HLA-A*6801 and HLA-A*0201 as viewed in profile from the peptide N-terminus toward the C-terminus (up is toward the T cell receptor, down is toward the floor of the peptide binding groove, left is toward the α1 helix domain, and right is toward the α2 helix domain). The residues at position 6 of the peptides with different orientations between HLA-A*6802 and HLA-A*0201 are marked with red rectangle. (F) The magnified view of the residues in the middle part of the peptides presented by HLA-A*6802, HLA-A*6801 and HLA-A*0201. Asn6 of peptide Env199 in HLA-A*6802/Env199 and Ser6 in peptide RT313 in HLA-A*6801/RT313 bind to the residues Gln70 and Thr73 through hydrogen bonds. No direct interact is observed between Asn6 of Env199 in HLA-A*0201/Env199 with the residues on the α1 helix of HLA-A2.

on our structures of HLA-A*6802, HLA-A*6801 and the previous determined HLA-A*0201/Env199, comparative analysis indicated that the similar hydrophobic residues Tyr7, Tyr9 (Phe9 for HLA-A*0201), Ala24, Val34, Val67 form the bottom of the B pocket of HLA-A*6802, HLA-A*6801, and HLA-A*0201 which adopt the side chain of the P2 anchor (Fig. 5A–C). However, the HLA-A*0201 has a small B pocket entrance compared to HLA-A*6802 and HLA-A*6801. A salt bridge at the edge of B pocket of HLA-A*0201 was observed between the two polymorphic residues Glu63 and Lys66 for HLA-A*0201 (Fig. 5D). Although the polymorphism of the residues at these two positions may not impact the P2 anchor selection of HLA-A*6802, HLA-A*6801, and HLA-A*0201, the exposing of the two residues to solvent may influences the TCR-docking at this region of the MHC. This may contribute to the distinct MHC-restricted TCR recognition of HLA-A*6802/HLA-A*6801, compared to HLA-A*0201. Actually, the polymorphic residues at position 63 between HLA-A*6802 and HLA-A*0201 also contribute to the different conformation of the P1 anchoring of peptide Env199 in the two related structures (Fig. 5D). In the structure of HLA-A*0201/Env199, a hydrogen bond is formed between Glu63 of heavy chain and P1 anchor Thr of Env199. However, no hydrogen bond is observed between Gln63 and P1 anchor Thr of Env199 in the structure of HLA-A*6802/Env199 (Table 2). This also indicates a subtle impact of the micropolymorpism between HLA-A*6802/HLA-A*6801 and HLA-A*0201 on their peptide presentation and T cell recognition.

3.5. Unconventional peptide presentation of HLA-A*6802 revealed by a distinct P3–Tyr anchoring of TRP2-180

In order to further demonstrate and confirm the peptide presentation strategies of HLA-A*6802, we determined another structure of HLA-A*6802 complexed with self peptide TRP2-180 derived from a tumor antigen TRP2. The overall structure of HLA-A*6802/TRP2-180 and the conformation of peptide TRP2-180 are similar to the one in structure of HLA-A*6802/Env199 with a RMSD of 0.583 Å. However, when we compare the structures of HLA-A*6802/TRP2-180 with all the HLA-A*0201 structures available on the PDB, we found that Tyr3 of TRP2-180, which acts as a secondary anchor residue, uncommonly inserts its side chain into the C pocket of HLA-A*6802. Instead, D pocket of HLA-A*6802 accommodates Phe5 of peptide TRP2-180. In contrast, the D pocket of HLA-A*0201 accommodates the P3 residues in all of the HLA-A*0201-presented peptides to the best of our knowledge (Fig. 6A).

Further structural analysis demonstrated that the Tyr3 of TRP2-180 forms a hydrogen bond with Gln70 of the α1-helix of HLA-A*6802, which corresponds to a polymorphic residue, His70, in HLA-A*0201 (Fig. 6B). This illuminates the contribution of allele-specific micropolymorphisms to the unconventional P3 Tyr anchoring of HLA-A*6802 presented peptide. A previous study indicates that the peptides presented by the HLA alleles from the A2 supertype prefer aromatic amino acids such as Tyr as secondary anchors at the P3 position (Sidney et al., 2001). Herein, base on the structure of HLA-A*6802/TRP2-180, a different binding mode for the P3 Tyr anchor of HLA-A*6802 is displayed when compared to other A2 supertype members (Liu et al., 2011a). In accord with the unusual P3 Tyr anchoring, the middle portion of the peptide binding groove of HLA-A*6802/TRP2-180 is wider than HLA-A*0201 (Fig. 6C), and a larger and deeper C pocket can be observed within the groove of HLA-A*6802 (Fig. 6D and E). This may be associated with the uncommon anchoring conformation of P3 Tyr which repels the underside and flank of C pocket of HLA-A*6802 peptide binding groove.

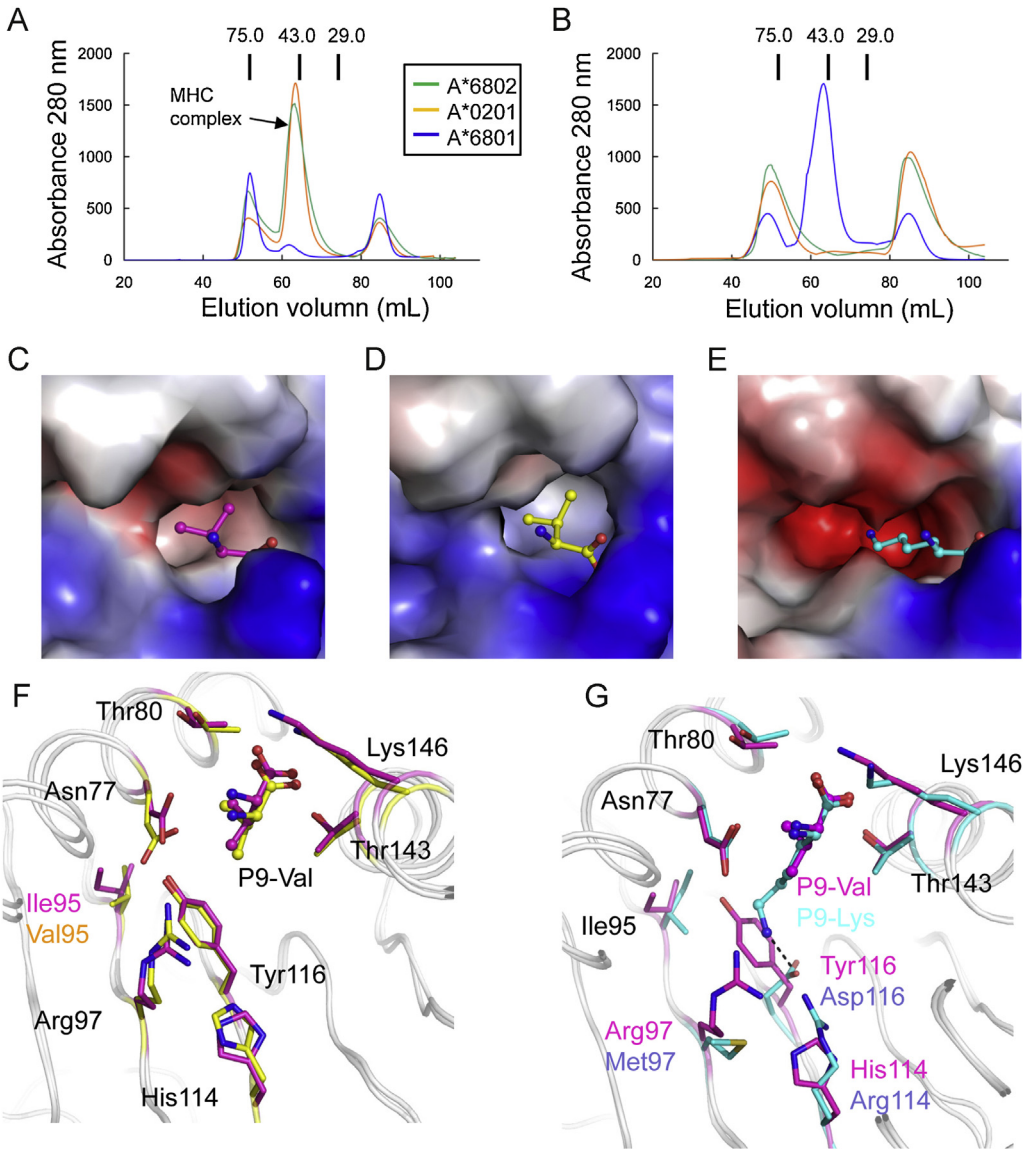

Fig. 4. The binding peptide motif of HLA-A*6802 is similar to HLA-A*0201 but not HLA-A*6801, determined by the properties of the F pockets. A and B. Binding of Env199 (A) and RT313 (B) to HLA-A*6802, HLA-A*6801, and HLA-A*0201 is elucidated by in vitro refolding. Peptides with the ability to bind to the HLA help the HLA heavy chain and β_2m refold in vitro. After properly refolding, we found that high-absorbance peaks of the MHCs with the expected molecular mass of 45 kDa eluted at the estimated volume of 65 ml on a Superdex® 75 10/300 GL column (GE Healthcare). The profile is marked with the approximate positions of the molecular mass standards of 75.0, 43.0, and 29.0 kDa. Complexes were formed by refolding of peptide Env199 with HLA-A*6802 and HLA-A*0201 but not with HLA-A*6801. On the contrary, peptide RT313 aided HLA-A*6801 renature into a soluble complex but displayed no binding to HLA-A*6802 or HLA-A*0201. C–E. Vacuum electrostatic surface potential shows that the F pockets of HLA-A*6802 (C) and HLA-A*0201 (D) are hydrophobic, which differs from the negatively charged F pocket of HLA-A*6801 (E). The Pc anchor residues are represented in sticks and balls with different colors (purple for HLA-A*6802-presented Env199, yellow for HLA-A*0201-presented Env199 in 1HHG, and cyan for HLA-A*6801-presented RT313). (F) Comparison of the F pocket residues of HLA-A*6802 and HLA-A*0201. The heavy chains are represented as gray loops. The major residues (purple sticks) of the F pocket of HLA-A*6802 have the same conformation as the corresponding residues (yellow sticks) of HLA-A*0201. The Pc residue Val of Env199 presented by HLA-A*6802 and HLA-A*0201, respectively, are shown in purple and yellow sticks and balls. (G) Distinct F pockets of HLA-A*6802 and HLA-A*6801. The residues of the HLA-A*6801 heavy chain are represented in cyan. The Pc Val of the HLA-A*6802-bound peptide Env199 and the Pc Lys of the HLA-A*6801-bound peptide RT313 are shown as purple and cyan sticks and balls, respectively. The salt bridge between the Pc Lys of RT313 and Asp116 of the HLA-A*6801 F pocket is represented as black dashed lines. In (F) and (G), the names of residues that are similar between HLA-A*6802 and HLA-A*0201 or between HLA-A*6802 and HLA-A*6801 are labeled in black; the different ones are labeled according to the colors of the residues.

4. Discussion

Our studies demonstrate that HLA-A*6802 possesses a similar overall structure to HLA-A*6801, indicating an identical serotype classification. However, the conformations of the polymorphic residues within the peptide binding groove of HLA-A*6802, especially the F pocket, are distinct from HLA-A*6801 but similar to HLA-A*0201. This determines the A2 supertype-like peptide binding motif of HLA-A*6802 as HLA-A*0201. Interestingly, the peptide presentation strategy of HLA-A*6802, e.g. the conformations of the N terminal and the middle portion of the peptide, are more homologous to HLA-A*6801 compared to HLA-A*0201. Therefore, our comparative structural analyses of HLA-A*6802 and HLA-A*6801 together with HLA-A*0201 indicate an unusual peptide presentation feature of HLA-A*6802 (Doytchinova and Flower, 2003), which may imply a unique pathogen specific T cell recognition within HLA-A*6802$^+$ populations (Hogan et al., 1998; Rowland-Jones et al., 1998).

Previous experimental and bioinformatic studies have indicated that there are still many other HLA-A alleles (e.g. HLA-A*6815,

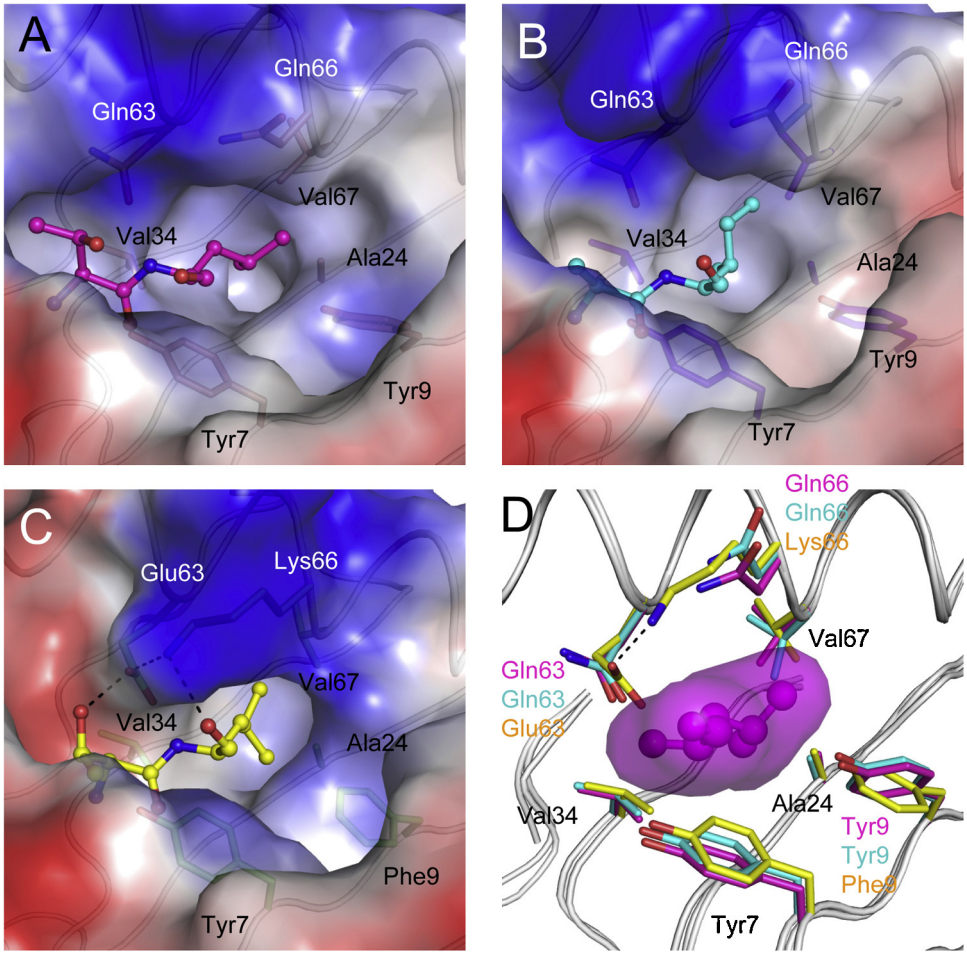

Fig. 5. Similar B pockets of HLA-A*6802 with HLA-A*6801 other than HLA-A*0201. (A–C) Vacuum electrostatic surface potential of the B pockets of HLA-A*6802 (A), HLA-A*6801 (B), and HLA-A*0201 (C) with the P1 and P2 resides of the peptides (stick and sphere) in the pockets. The major residues composing the B pockets of the HLAs are shown as sticks. Within the B pocket of HLA-A*0201 (C), the salt bridge that extends over the edge of B pocket is formed by the Glu63 and Lys66. Hydrogen bonds between the peptide residue and the α1 helix are also observed (black dashed lines). (D) Comparison of the B pocket residues of HLA-A*6802 (purple), HLA-A*6801 (cyan), and HLA-A*0201 (yellow). The heavy chains are represented as gray loops. The major residues of the B pocket of the three alleles are in the same conformation. The polymorphic residues Glu63 and Lys66 of HLA-A*0201 form the salt bridge (black dashed lines) which is different from HLA-A*6802 and HLA-A*6801. The names of residues that are similar between HLA-A*6802, HLA-A*6801, and HLA-A*0201 are labeled in black; the different ones are labeled according to the colors of the residues. The position of the P2 anchors of the peptides presented by these three alleles are represented by the P2 Leu of HLA-A*6801/Env199 shown in purple sticks and spheres with surfaces.

HLA-A*6827, HLA-A*6828, and HLA-A*6901, etc.) within the A2 supertype (Sidney et al., 2008), which present the typical A2 restricted peptides (or have the A2 supertype polymorphic residues) but belong to the HLA-A68 or HLA-A69 serotypes (both are the subtypes of the common African broad antigen serotype A28) (Fig. 2B) (Fernandez-Vina et al., 1992; Hsu et al., 1999; Krausa et al., 1993). Detailed sequence and structure analyses indicated that these alleles posses the A2 supertype specific residues (as Arg97, His114, and Tyr116) in F pocket, as HLA-A*6802 (Fig. 2A). However, within the B and C pockets, these HLA-A*6802-like alleles bear residues (e.g. Gln63, Gln66, and Asn70) which are distinct from typical A2 alleles (HLA-A2 serotype alleles, such as HLA-A*0201 to HLA-A*0207). The hybrid micropolymorphism of these HLA-A*6802-like alleles may lead to a featured peptide presentation characteristic as HLA-A*6802. Therefore, based on the structural properties of the micropolymorphism and potential different peptide presentations, the A2 supertype can be divided into two groups: Group1: HLA-A*0201-like (e.g. HLA-A*0201–0207, etc.) and Group2: HLA-A*6802-like alleles (e.g. HLA-A*6815, HLA-A*6827, HLA-A*6828, and HLA-A*6901, etc.). These two groups can present the peptides with similar motif at P2 and Pc positions but in subtle different conformations. A recent structural study elucidated the peptide presentation features of four HLA-A*0201-like molecules: HLA-A*0201, HLA-A*0203, HLA-A*0206, and HLA-A*0207(Liu et al., 2011a). Herein our structures of HLA-A*6802 provide the insights into the peptide presentation of the HLA-A*6802-like group. Peptides with similar A2 supertype restricted motif can be presented by these two groups, but in different conformations. Furthermore, the TCR restriction may also differ between these two groups due to the polymorphic residues within the solvent-exposing region of α1 and α2 helixes. However, experimental exploration is needed to confirm the peptide binding and the TCR recognition features of A2 supertype alleles in a broader manner.

In spite of the micropolymorphism modulated different peptide presentations, many studies illuminated a common phenomenon of the cross-allele presentation of similar peptides by HLA-A*0201-like and HLA-A*6802-like alleles. Mitchell et al. reported that within six naturally displayed HLA-A2.1-restricted melanoma specific CTL epitopes, four of the epitopes can also be recognized in the HLA-A*6802 context by the cross-reactive CTLs (Mitchell et al., 2000). It is also indicated that HLA A2-restricted Epstein–Barr virus-specific CTLs were able to lyse EBV-infected B cells expressing different HLA A2 supertype alleles including A*0201, A*0202, A*0203, A*0204, A*0206, A*6802 and A*6901 (Khanna et al., 1998). These findings indicated that although the peptide presentation of alleles (as HLA-A*0201 and HLA-A*6802) within the A2 supertype can

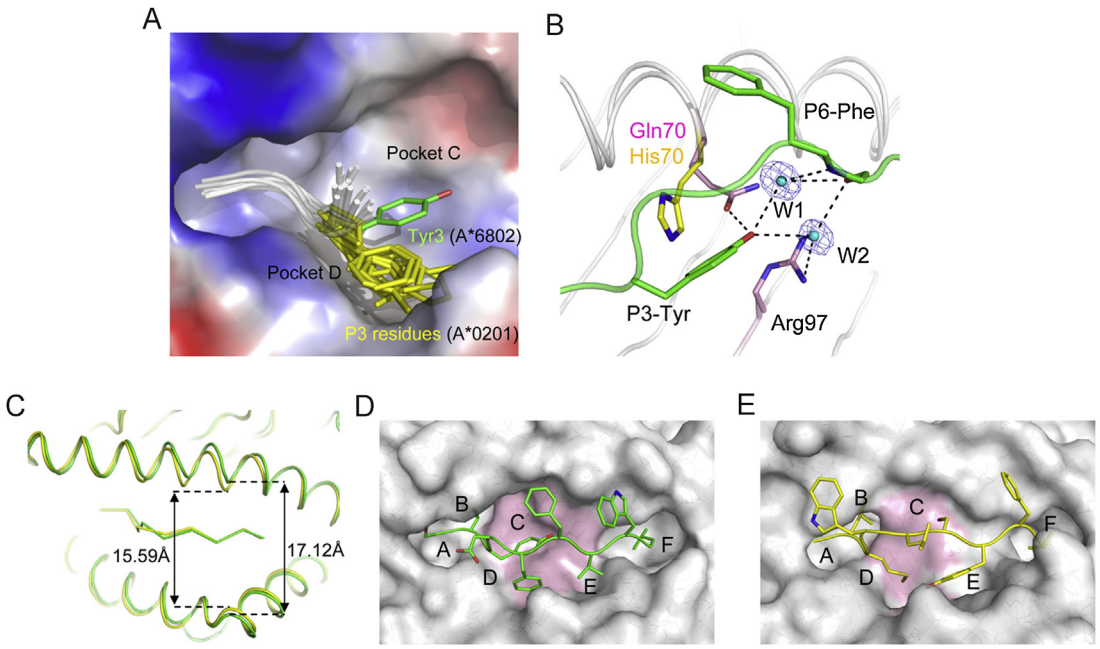

Fig. 6. Unconventional P3-Tyr anchoring of TRP2-180 presented by HLA-A*6802. (A) Alignment of TRP2-180 presented by HLA-A*6802 with peptides presented by HLA-A*0201 indicates that the P3 residue Tyr (green) of the HLA-A*6802-bound peptide occupies the C pocket, whereas P3 residues (yellow) of all of the HLA-A*0201-bound peptides insert their side chains into the D pocket. The HLA-A*0201 structures shown here are 1AKJ, 1AO7, 1B0R, 1HHG, 1HHI, 1HHJ, 1HHK, 1JF1, 1JHT, 1P7Q, 1QRN, 1S8D, 1S9W, 1T1X, 1T1Z, 1TVB, 2C7U, 2J8U, 2VLJ and 3I6G. Different mutations of the peptides are not included. (B) Interactions of the P3 Tyr of peptide TRP2-180 with the residues within the C pocket of HLA-A*6802. The P3 Tyr interacts (black dashed lines) with Gln70 and Arg97 through hydrogen bonds and water linkage. The polymorphic residues Gln and His at position 70 of HLA-A*6802 and HLA-A*0201 are denoted in pink and yellow sticks, respectively. Uncommon intra-chain interactions via two water molecules are also observed between the P3 Tyr and P7 Val of TRP2-180 (Liu et al., 2010b). The existence of the two water molecules is clearly shown by electron density at the 1.0σ contour level. (C) The peptide binding groove of HLA-A*6802 (green) is wider than HLA-A*0201 (yellow) at the middle portion where the C pocket is located. The distances are measured between the Cα of Thr73 and Ala150 of the molecules HLA-A*6802/TRP2-180 and HLA-A*0201/Env199, respectively. (D and E) The surfaces of the peptide-binding grooves of HLA-A*6802 and HLA-A*0201 are shown in gray, and the peptides TRP2-180 and Env199 from the structures of HLA-A*6802 (D) and HLA-A*0201 (E) are represented as green or yellow stick models. The pink surface indicates a larger and deeper C pocket in HLA-A*6802 compared to HLA-A*0201. Pockets A to F are labeled in black letters. The C and D pockets of HLA-A*6802 accommodate the side chains of the P3 Tyr and P4 Phe of TRP2-180, respectively (D). The P3 Met of peptide Env199 points into the D pocket of HLA-A*0201 (E).

be subtly modulated by the micropolymorphism, similar peptides can still be presented by these alleles and subsequently induce cross T cell responses in different HLA allele individuals. The existence of the cross-reactive CTLs can be comprehended through the recent concept of the promiscuity of CTL recognition established by the broadly structure determination of cross-reactive TCRs and the related MHC complexes (Borbulevych et al., 2009; Lichterfeld et al., 2006; Liu et al., 2012; Mongkolsapaya et al., 2006; Yin and Mariuzza, 2009). In addition, the similar processing and transportation of the antigenic peptides within the antigen presenting cells (APCs) within different HLA alleles is also a prerequisite for the peptide cross-allele presentation and recognition (Walker et al., 2011).

In previous study, we have identified a SARS coronavirus-derived $CD8^+$ T cell epitope N1 which is presented by HLA-A*2402 in an uncommon strategy (Liu et al., 2010b). A dramatically similar overall conformation is observed between the two peptides presented by HLA-A*6802 and HLA-A*2402 (data not shown). Similar to our structure of HLA-A*6802/TRP2-180, the Lys3 residue of peptide N1 in the HLA-A*2402 structure also locates in the C pocket but not D pocket in the peptide binding groove. In HLA-A*6802/TRP2-180, Gln70 of the α1-helix of HLA-A*6802 grabs Tyr3 of peptide TRP2-180 through a hydrogen bond. Interestingly, for N1 presented by HLA-A*2402, intrachain hydrogen bonds between Lys3 and Gln5 is formed which stabilizes the main chain conformation of N1. Due to the hydrogen bonds contributed by the P3 anchor in C pocket, both of peptides TRP2-180 and N1 display a bulged conformation, in which the residues in the middle portion of the peptides protrude out of the peptide binding grooves. This bulged peptide conformation within HLA-A*6802/TRP2-180 and HLA-A*2402/N1 helps to expose the amino acids in middle region of the peptide for the TCR docking in T cell recognition.

The comparative structural characterization of peptide presentation of HLA-A*6802, HLA-A*6801, and HLA-A*0201 illuminates a molecular basis for their A2 and A3 supertype differentiation and demonstrates the rationality of the supertype classification of HLA alleles based on binding-peptide motif. Moreover, these findings also provide beneficial reference points for viruses and tumors specific T-cell recognition of broadly cross-allele presented peptide, but still delicately restricted by polymorphic HLA. Given the prevalence of the HLA-$A68^+$ population in Africa and the close correlation of A2-A*6802 supertype in HIV resistance, our study may shed light on the T cell vaccine development of HIV.

Conflict-of-interest

The authors declare no financial or commercial conflicts of interest.

Acknowledgements

This work was supported by the China National Grand S&T Special Project (No. 2013ZX10004608), the National Natural Science Foundation of China (NSFC, No. 31030030), and the 973 Project of the China Ministry of Science and Technology (MOST, No. 2010CB911902), and the funders had no role in study design, data collection and analysis, decision to publish, or preparation of the manuscript. GFG is a leading principal investigator of the NSFC Innovative Research Group (Grant No. 81021003).

We thank Dr. Yi Shi and Ms. Meng Cheng for their excellent assistance and suggestion in the project.

Appendix A. Supplementary data

Supplementary data associated with this article can be found, in the online version, at http://dx.doi.org/10.1016/j.molimm.2013.03.015.

References

Adams, P.D., Afonine, P.V., Bunkoczi, G., Chen, V.B., Davis, I.W., Echols, N., Headd, J.J., Hung, L.W., Kapral, G.J., Grosse-Kunstleve, R.W., McCoy, A.J., Moriarty, N.W., Oeffner, R., Read, R.J., Richardson, D.C., Richardson, J.S., Terwilliger, T.C., Zwart, P.H., 2010. PHENIX: a comprehensive Python-based system for macromolecular structure solution. Acta Crystallographica. Section D: Biological Crystallography 66, 213–221.

Arnett, K.L., Parham, P., 1995. HLA class I nucleotide sequences, 1995. Tissue Antigens 46, 217–257.

Barouch, D., Friede, T., Stevanovic, S., Tussey, L., Smith, K., Rowland-Jones, S., Braud, V., McMichael, A., Rammensee, H.G., 1995. HLA-A2 subtypes are functionally distinct in peptide binding and presentation. Journal of Experimental Medicine 182, 1847–1856.

Bjorkman, P.J., Saper, M.A., Samraoui, B., Bennett, W.S., Strominger, J.L., Wiley, D.C., 1987. Structure of the human class I histocompatibility antigen, HLA-A2. Nature 329, 506–512.

Borbulevych, O.Y., Piepenbrink, K.H., Gloor, B.E., Scott, D.R., Sommese, R.F., Cole, D.K., Sewell, A.K., Baker, B.M., 2009. T cell receptor cross-reactivity directed by antigen-dependent tuning of peptide-MHC molecular flexibility. Immunity 31, 885–896.

Brunger, A.T., Adams, P.D., Clore, G.M., DeLano, W.L., Gros, P., Grosse-Kunstleve, R.W., Jiang, J.S., Kuszewski, J., Nilges, M., Pannu, N.S., Read, R.J., Rice, L.M., Simonson, T., Warren, G.L., 1998. Crystallography & NMR system: a new software suite for macromolecular structure determination. Acta Crystallographica. Section D: Biological Crystallography 54, 905–921.

Chen, H., Ndhlovu, Z.M., Liu, D., Porter, L.C., Fang, J.W., Darko, S., Brockman, M.A., Miura, T., Brumme, Z.L., Schneidewind, A., Piechocka-Trocha, A., Cesa, K.T., Sela, J., Cung, T.D., Toth, I., Pereyra, F., Yu, X.G., Douek, D.C., Kaufmann, D.E., Allen, T.M., Walker, B.D., 2012. TCR clonotypes modulate the protective effect of HLA class I molecules in HIV-1 infection. Nature Immunology 13, 691–700.

Conway, D.J., Holland, M.J., Bailey, R.L., Campbell, A.E., Mahdi, O.S., Jennings, R., Mbena, E., Mabey, D.C., 1997. Scarring trachoma is associated with polymorphism in the tumor necrosis factor alpha (TNF-alpha) gene promoter and with elevated TNF-alpha levels in tear fluid. Infection and Immunity 65, 1003–1006.

Conway, D.J., Holland, M.J., Campbell, A.E., Bailey, R.L., Krausa, P., Peeling, R.W., Whittle, H.C., Mabey, D.C., 1996. HLA class I and II polymorphisms and trachomatous scarring in a Chlamydia trachomatis-endemic population. Journal of Infectious Diseases 174, 643–646.

de Bakker, P.I., McVean, G., Sabeti, P.C., Miretti, M.M., Green, T., Marchini, J., Ke, X., Monsuur, A.J., Whittaker, P., Delgado, M., Morrison, J., Richardson, A., Walsh, E.C., Gao, X., Galver, L., Hart, J., Hafler, D.A., Pericak-Vance, M., Todd, J.A., Daly, M.J., Trowsdale, J., Wijmenga, C., Vyse, T.J., Beck, S., Murray, S.S., Carrington, M., Gregory, S., Deloukas, P., Rioux, J.D., 2006. A high-resolution HLA and SNP haplotype map for disease association studies in the extended human MHC. Nature Genetics 38, 1166–1172.

del Guercio, M.F., Sidney, J., Hermanson, G., Perez, C., Grey, H.M., Kubo, R.T., Sette, A., 1995. Binding of a peptide antigen to multiple HLA alleles allows definition of an A2-like supertype. Journal of Immunology 154, 685–693.

Doytchinova, I., Flower, D., 2003. The HLA-A2-supermotif: a QSAR definition. Organic and Biomolecular Chemistry 1, 2648–2654.

Doytchinova, I.A., Flower, D.R., 2002. A comparative molecular similarity index analysis (CoMSIA) study identifies an HLA-A2 binding supermotif. Journal of Computer-Aided Molecular Design 16, 535–544.

Doytchinova, I.A., Guan, P., Flower, D.R., 2004a. Identifiying human MHC supertypes using bioinformatic methods. Journal of Immunology 172, 4314–4323.

Doytchinova, I.A., Guan, P., Flower, D.R., 2004b. Quantitative structure-activity relationships and the prediction of MHC supermotifs. Methods 34, 444–453.

Emsley, P., Cowtan, K., 2004. Coot: model-building tools for molecular graphics. Acta Crystallographica. Section D: Biological Crystallography 60, 2126–2132.

Fernandez-Vina, M.A., Falco, M., Sun, Y., Stastny, P., 1992. DNA typing for HLA class I alleles: I subsets of HLA-A2 and of -A28. Human Immunology 33, 163–173.

Fogg, M.H., Wirth, L.J., Posner, M., Wang, F., 2009. Decreased EBNA-1-specific $CD8^+$ T cells in patients with Epstein–Barr virus-associated nasopharyngeal carcinoma. Proceedings of the National Academy of Sciences of the United States of America 106, 3318–3323.

Frahm, N., Baker, B., Brander, C., 2008. Identification and optimal definition of HIV-derived cytotoxic T lymphocyte (CTL) epitopes for the study of CTL escape, functional avidity and viral evolution. HIV Molecular Immunology 2008, 3–24.

Gao, G.F., Willcox, B.E., Wyer, J.R., Boulter, J.M., O'Callaghan, C.A., Maenaka, K., Stuart, D.I., Jones, E.Y., Van Der Merwe, P.A., Bell, J.I., Jakobsen, B.K., 2000. Classical and nonclassical class I major histocompatibility complex molecules exhibit subtle conformational differences that affect binding to CD8alphaalpha. Journal of Biological Chemistry 275, 15232–15238.

Garboczi, D.N., Hung, D.T., Wiley, D.C., 1992. HLA-A2-peptide complexes: refolding and crystallization of molecules expressed in *Escherichia coli* and complexed with single antigenic peptides. Proceedings of the National Academy of Sciences of the United States of America 89, 3429–3433.

Gostick, E., Cole, D.K., Hutchinson, S.L., Wooldridge, L., Tafuro, S., Laugel, B., Lissina, A., Oxenius, A., Boulter, J.M., Price, D.A., Sewell, A.K., 2007. Functional and biophysical characterization of an HLA-A*6801-restricted HIV-specific T cell receptor. European Journal of Immunology 37, 479–486.

Goulder, P.J., Walker, B.D., 2012. HIV and HLA class I: an evolving relationship. Immunity 37, 426–440.

Guan, P., Doytchinova, I.A., Flower, D.R., 2003. HLA-A3 supermotif defined by quantitative structure-activity relationship analysis. Protein Engineering 16, 11–18.

Guo, H.C., Jardetzky, T.S., Garrett, T.P., Lane, W.S., Strominger, J.L., Wiley, D.C., 1992. Different length peptides bind to HLA-Aw68 similarly at their ends but bulge out in the middle. Nature 360, 364–366.

Guo, H.C., Madden, D.R., Silver, M.L., Jardetzky, T.S., Gorga, J.C., Strominger, J.L., Wiley, D.C., 1993. Comparison of the P2 specificity pocket in three human histocompatibility antigens: HLA-A*6801, HLA-A*0201, and HLA-B*2705. Proceedings of the National Academy of Sciences of the United States of America 90, 8053–8057.

Hattotuwagama, C.K., Doytchinova, I.A., Flower, D.R., 2007. Toward the prediction of class I and II mouse major histocompatibility complex-peptide-binding affinity: in silico bioinformatic step-by-step guide using quantitative structure-activity relationships. Methods in Molecular Biology 409, 227–245.

Hogan, K.T., Eisinger, D.P., Cupp 3rd, S.B., Lekstrom, K.J., Deacon, D.D., Shabanowitz, J., Hunt, D.F., Engelhard, V.H., Slingluff Jr., C.L., Ross, M.M., 1998. The peptide recognized by HLA-A68.2-restricted, squamous cell carcinoma of the lung-specific cytotoxic T lymphocytes is derived from a mutated elongation factor 2 gene. Cancer Research 58, 5144–5150.

Hsu, E., Bei, M., Slack, R., Hartzman, R.J., Ng, J., Hurley, C.K., 1999. HLA-A*28 allele frequencies in the five major U.S. ethnic groups. Human Immunology 60, 159–167.

Khanna, R., Burrows, S.R., Nicholls, J., Poulsen, L.M., 1998. Identification of cytotoxic T cell epitopes within Epstein–Barr virus (EBV) oncogene latent membrane protein 1 (LMP1): evidence for HLA A2 supertype-restricted immune recognition of EBV-infected cells by LMP1-specific cytotoxic T lymphocytes. European Journal of Immunology 28, 451–458.

Koch, M., Camp, S., Collen, T., Avila, D., Salomonsen, J., Wallny, H.J., van Hateren, A., Hunt, L., Jacob, J.P., Johnston, F., Marston, D.A., Shaw, I., Dunbar, P.R., Cerundolo, V., Jones, E.Y., Kaufman, J., 2007. Structures of an MHC class I molecule from B21 chickens illustrate promiscuous peptide binding. Immunity 27, 885–899.

Krausa, P., Bodmer, J.G., Browning, M.J., 1993. Defining the common subtypes of HLA A9, A10, A28 and A19 by use of ARMS/PCR. Tissue Antigens 42, 91–99.

Laskowski, R.A., Macarthur, M.W., Moss, D.S., Thornton, J.M., 1993. Procheck – a program to check the stereochemical quality of protein structures. Journal of Applied Crystallography 26, 283–291.

Li, L., Bouvier, M., 2004. Structures of HLA-A*1101 complexed with immunodominant nonamer and decamer HIV-1 epitopes clearly reveal the presence of a middle, secondary anchor residue. Journal of Immunology 172, 6175–6184.

Li, X., Liu, J., Qi, J., Gao, F., Li, Q., Li, X., Zhang, N., Xia, C., Gao, G.F., 2011. Two distinct conformations of a rinderpest virus epitope presented by bovine major histocompatibility complex class I N*01801: a host strategy to present featured peptides. Journal of Virology 85, 6038–6048.

Lichterfeld, M., Williams, K.L., Mui, S.K., Shah, S.S., Mothe, B.R., Sette, A., Kim, A., Johnston, M.N., Burgett, N., Frahm, N., Cohen, D., Brander, C., Rosenberg, E.S., Walker, B.D., Altfeld, M., Yu, X.G., 2006. T cell receptor cross-recognition of an HIV-1 $CD8^+$ T cell epitope presented by closely related alleles from the HLA-A3 superfamily. International Immunology 18, 1179–1188.

Liu, J., Chen, K.Y., Ren, E.C., 2011a. Structural insights into the binding of hepatitis B virus core peptide to HLA-A2 alleles: towards designing better vaccines. European Journal of Immunology 41, 2097–2106.

Liu, J., Dai, L., Qi, J., Gao, F., Feng, Y., Liu, W., Yan, J., Gao, G.F., 2011b. Diverse peptide presentation of rhesus macaque major histocompatibility complex class I Mamu-A 02 revealed by two peptide complex structures and insights into immune escape of simian immunodeficiency virus. Journal of Virology 85, 7372–7383.

Liu, J., Sun, Y., Qi, J., Chu, F., Wu, H., Gao, F., Li, T., Yan, J., Gao, G.F., 2010a. Membrane protein of SARS-CoV acts as a dominant immunogen revealed by a clustering region of novel functional and structural defined CTL epitopes. Journal of Infectious Diseases 202, 1171–1180.

Liu, J., Wu, P., Gao, F., Qi, J., Kawana-Tachikawa, A., Xie, J., Vavricka, C.J., Iwamoto, A., Li, T., Gao, G.F., 2010b. Novel immunodominant peptide presentation strategy: a featured HLA-A*2402-restricted cytotoxic T-lymphocyte epitope stabilized by intrachain hydrogen bonds from severe acute respiratory syndrome coronavirus nucleocapsid protein. Journal of Virology 84, 11849–11857.

Liu, J., Zhang, S., Tan, S., Yi, Y., Wu, B., Cao, B., Zhu, F., Wang, C., Wang, H., Qi, J., Gao, G.F., 2012. Cross-allele cytotoxic T lymphocyte responses against 2009 pandemic H1N1 influenza A virus among HLA-A24 and HLA-A3 supertype-positive individuals. Journal of Virology 86, 13281–13294.

Liu, J., Zhang, S., Tan, S., Zheng, B., Gao, G.F., 2011c. Revival of the identification of cytotoxic T-lymphocyte epitopes for immunological diagnosis, therapy and vaccine development. Experimental Biology and Medicine (Maywood, NJ) 236, 253–267.

Longmate, J., York, J., La Rosa, C., Krishnan, R., Zhang, M., Senitzer, D., Diamond, D.J., 2001. Population coverage by HLA class-I restricted cytotoxic T-lymphocyte epitopes. Immunogenetics 52, 165–173.

Lund, O., Nielsen, M., Kesmir, C., Petersen, A.G., Lundegaard, C., Worning, P., Sylvester-Hvid, C., Lamberth, K., Roder, G., Justesen, S., Buus, S., Brunak, S., 2004. Definition of supertypes for HLA molecules using clustering of specificity matrices. Immunogenetics 55, 797–810.

MacDonald, K.S., Embree, J.E., Nagelkerke, N.J., Castillo, J., Ramhadin, S., Njenga, S., Oyug, J., Ndinya-Achola, J., Barber, B.H., Bwayo, J.J., Plummer, F.A., 2001a. The HLA A2/6802 supertype is associated with reduced risk of perinatal human immunodeficiency virus type 1 transmission. The Journal of Infectious Diseases 183, 503–506.

MacDonald, K.S., Fowke, K.R., Kimani, J., Dunand, V.A., Nagelkerke, N.J., Ball, T.B., Oyugi, J., Njagi, E., Gaur, L.K., Brunham, R.C., Wade, J., Luscher, M.A., Krausa, P., Rowland-Jones, S., Ngugi, E., Bwayo, J.J., Plummer, F.A., 2000. Influence of HLA supertypes on susceptibility and resistance to human immunodeficiency virus type 1 infection. Journal of Infectious Diseases 181, 1581–1589.

MacDonald, K.S., Matukas, L., Embree, J.E., Fowke, K., Kimani, J., Nagelkerke, N.J., Oyugi, J., Kiama, P., Kaul, R., Luscher, M.A., Rowland-Jones, S., Ndinya-Achola, J., Ngugi, E., Bwayo, J.J., Plummer, F.A., 2001b. Human leucocyte antigen supertypes and immune susceptibility to HIV-1, implications for vaccine design. Immunology Letters 79, 151–157.

Madden, D.R., Garboczi, D.N., Wiley, D.C., 1993. The antigenic identity of peptide-MHC complexes: a comparison of the conformations of five viral peptides presented by HLA-A2. Cell 75, 693–708.

Marsh, S.G., Albert, E.D., Bodmer, W.F., Bontrop, R.E., Dupont, B., Erlich, H.A., Fernandez-Vina, M., Geraghty, D.E., Holdsworth, R., Hurley, C.K., Lau, M., Lee, K.W., Mach, B., Maiers, M., Mayr, W.R., Muller, C.R., Parham, P., Petersdorf, E.W., Sasazuki, T., Strominger, J.L., Svejgaard, A., Terasaki, P.I., Tiercy, J.M., Trowsdale, J., 2010. Nomenclature for factors of the HLA system, 2010. Tissue Antigens 75, 291–455.

Mitchell, M.S., Kan-Mitchell, J., Minev, B., Edman, C., Deans, R.J., 2000. A novel melanoma gene (MG50) encoding the interleukin 1 receptor antagonist and six epitopes recognized by human cytolytic T lymphocytes. Cancer Research 60, 6448–6456.

Mongkolsapaya, J., Duangchinda, T., Dejnirattisai, W., Vasanawathana, S., Avirutnan, P., Jairungsri, A., Khemnu, N., Tangthawornchaikul, N., Chotiyarnwong, P., Sae-Jang, K., Koch, M., Jones, Y., McMichael, A., Xu, X., Malasit, P., Screaton, G., 2006. T cell responses in dengue hemorrhagic fever: are cross-reactive T cells suboptimal? Journal of Immunology 176, 3821–3829.

Murshudov, G.N., Vagin, A.A., Dodson, E.J., 1997. Refinement of macromolecular structures by the maximum-likelihood method. Acta Crystallographica. Section D: Biological Crystallography 53, 240–255.

Naugler, C., Liwski, R., 2008. An evolutionary approach to major histocompatibility diversity based on allele supertypes. Medical Hypotheses 70, 933–937.

Ngandu, N.K., Seoighe, C., Scheffler, K., 2009. Evidence of HIV-1 adaptation to host HLA alleles following chimp-to-human transmission. Virology Journal 6, 164.

Ojesina, A.I., Sankale, J.L., Odaibo, G., Langevin, S., Meloni, S.T., Sarr, A.D., Olaleye, D., Kanki, P.J., 2006. Subtype-specific patterns in HIV Type 1 reverse transcriptase and protease in Oyo State, Nigeria: implications for drug resistance and host response. AIDS Research and Human Retroviruses 22, 770–779.

Parkhurst, M.R., Fitzgerald, E.B., Southwood, S., Sette, A., Rosenberg, S.A., Kawakami, Y., 1998. Identification of a shared HLA-A*0201-restricted T-cell epitope from the melanoma antigen tyrosinase-related protein 2 (TRP2). Cancer Research 58, 4895–4901.

Reche, P.A., Reinherz, E.L., 2007. Definition of MHC supertypes through clustering of MHC peptide-binding repertoires. Methods in Molecular Biology 409, 163–173.

Rowland-Jones, S.L., Dong, T., Fowke, K.R., Kimani, J., Krausa, P., Newell, H., Blanchard, T., Ariyoshi, K., Oyugi, J., Ngugi, E., Bwayo, J., MacDonald, K.S., McMichael, A.J., Plummer, F.A., 1998. Cytotoxic T cell responses to multiple conserved HIV epitopes in HIV-resistant prostitutes in Nairobi. Journal of Clinical Investigation 102, 1758–1765.

Sette, A., Sidney, J., 1998. HLA supertypes and supermotifs: a functional perspective on HLA polymorphism. Current Opinion in Immunology 10, 478–482.

Sette, A., Sidney, J., 1999a. Nine major HLA class I supertypes account for the vast preponderance of HLA-A and -B polymorphism. Immunogenetics 50, 201–212.

Sette, A., Sidney, J., 1999b. Nine major HLA class I supertypes account for the vast preponderance of HLA-A and -B polymorphism. Immunogenetics 50, 201–212.

Sette, A., Sidney, J., Livingston, B.D., Dzuris, J.L., Crimi, C., Walker, C.M., Southwood, S., Collins, E.J., Hughes, A.L., 2003. Class I molecules with similar peptide-binding specificities are the result of both common ancestry and convergent evolution. Immunogenetics 54, 830–841.

Sidney, J., Grey, H.M., Southwood, S., Celis, E., Wentworth, P.A., del Guercio, M.F., Kubo, R.T., Chesnut, R.W., Sette, A., 1996. Definition of an HLA-A3-like supermotif demonstrates the overlapping peptide-binding repertoires of common HLA molecules. Human Immunology 45, 79–93.

Sidney, J., Peters, B., Frahm, N., Brander, C., Sette, A., 2008. HLA class I supertypes: a revised and updated classification. BMC Immunology 9, 1.

Sidney, J., Southwood, S., Mann, D.L., Fernandez-Vina, M.A., Newman, M.J., Sette, A., 2001. Majority of peptides binding HLA-A*0201 with high affinity crossreact with other A2-supertype molecules. Human Immunology 62, 1200–1216.

Tang, J., Tang, S., Lobashevsky, E., Myracle, A.D., Fideli, U., Aldrovandi, G., Allen, S., Musonda, R., Kaslow, R.A., Zambia, U.A.B.H.I.V.R.P., 2002. Favorable and unfavorable HLA class I alleles and haplotypes in Zambians predominantly infected with clade C human immunodeficiency virus type 1. Journal of Virology 76, 8276–8284.

Threlkeld, S.C., Wentworth, P.A., Kalams, S.A., Wilkes, B.M., Ruhl, D.J., Keogh, E., Sidney, J., Southwood, S., Walker, B.D., Sette, A., 1997. Degenerate and promiscuous recognition by CTL of peptides presented by the MHC class I A3-like superfamily: implications for vaccine development. Journal of Immunology 159, 1648–1657.

Walker B., McMichael A., 2011. The T-Cell Response to HIV. Cold Spring Harbor Perspectives in Medicine 2. http://dx.doi.org/10.1101/cshperspect.a007054

Walker, B.A., Hunt, L.G., Sowa, A.K., Skjodt, K., Gobel, T.W., Lehner, P.J., Kaufman, J., 2011. The dominantly expressed class I molecule of the chicken MHC is explained by coevolution with the polymorphic peptide transporter (TAP) genes. Proceedings of the National Academy of Sciences of the United States of America 108, 8396–8401.

Wu, Y., Gao, F., Liu, J., Qi, J., Gostick, E., Price, D.A., Gao, G.F., 2011. Structural basis of diverse peptide accommodation by the rhesus macaque MHC class I molecule Mamu-B*17: insights into immune protection from simian immunodeficiency virus. Journal of Immunology 187, 6382–6392.

Yin, Y., Mariuzza, R.A., 2009. The multiple mechanisms of T cell receptor cross-reactivity. Immunity 31, 849–851.

Zhang, S., Liu, J., Cheng, H., Tan, S., Qi, J., Yan, J., Gao, G.F., 2011. Structural basis of cross-allele presentation by HLA-A*0301 and HLA-A*1101 revealed by two HIV-derived peptide complexes. Molecular Immunology 49, 395–401.

Zhu, S., Udaka, K., Sidney, J., Sette, A., Aoki-Kinoshita, K.F., Mamitsuka, H., 2006. Improving MHC binding peptide prediction by incorporating binding data of auxiliary MHC molecules. Bioinformatics 22, 1648–1655.